Journal of Materials Chemistry C

Synthesis of a novel strontium-based wide-bandgap semiconductor via X-ray photochemistry at extreme conditions

Journal:	*Journal of Materials Chemistry C*
Manuscript ID	TC-COM-09-2018-004496.R1
Article Type:	Communication
Date Submitted by the Author:	30-Oct-2018
Complete List of Authors:	Evlyukhin, Egor; University of Nevada Las Vegas College of Sciences, Physics and Astronomy Kim, Eunja; University of Nevada Las Vegas, Physics and Astronomy Cifligu, Petrika; University of Nevada Las Vegas, Physics and Astronomy Goldberger, David; University of Nevada Las Vegas, Physics and Astronomy Schyck, Sarah; University of Nevada Las Vegas, Physics and Astronomy Harris, Blake; University of Nevada Las Vegas, Physics and Astronomy Torres, Sindi; University of Nevada Las Vegas, Physics and Astronomy Rossman, George; California Institute of Technology Division of Geological and Planetary Sciences Pravica, Michael; University of Nevada Las Vegas, Physics and Astronomy

Journal Name

COMMUNICATION

Synthesis of a novel strontium-based wide-bandgap semiconductor via X-ray photochemistry at extreme conditions†

Received 00th January 20xx,
Accepted 00th January 20xx

DOI: 10.1039/x0xx00000x

www.rsc.org/

Egor Evylukhin*[a], Eunja Kim [a], Petrika Cifligu [a], David Goldberger [a], Sarah Schyck [a], Blake Harris [a], Sindi Torres [a], George R. Rossman [b], and Michael Pravica [a]

The synthesis and characterization of a novel, low cost, amorphous wide-bandgap semiconductor via X-ray induced decomposition of strontium oxalate at high pressure is demonstrated. By means of IR spectroscopy, the final product is identified as a mixture of strontium carbonate, strontium oxalate and CO-derived materials. Band gap measurements demonstrate that the final product exhibits a much lower band gap (2.45 eV) than the initial strontium oxalate powder (4.07 eV), suggesting that the synthesized material can be highly useful in electronic and optical applications.

Amorphous semiconductors attract much attention because of their electron transport properties which are highly utilized in optoelectronic applications.[1] The absence of long-range order in amorphous systems can either substantially degrade the conductive properties (e.g. amorphous silicon) relative to the crystalline phase,[2] or increase the charge carrier mobility in the system (e.g. amorphous oxide semiconductors).[3] Although, there are two well developed principal techniques for the preparation of amorphous samples: (i) cooling from the melt and (ii) deposition on a substrate,[4] they both require precise control of many fabrication parameters for successful synthesis. For instance, in fabrication of multicomponent alloy glasses, the cooling rate is a critical parameter and depends on the material composition.[5,6] In the second case, deposition on a substrate or vapor quenching techniques for producing film samples strongly depend on the condensing surface temperature, deposition rates, purity, gas contaminates,[7-9] *etc*. Although, these techniques are efficient and widely used, the search for novel methods which require less control parameters for the efficient development of low cost, amorphous semiconductors with unique optical properties is still one of the main challenges of material science.

In this work, we demonstrate that X-rays with high pressure assistance can be a novel and powerful tool for producing amorphous semiconductors in bulk via decomposition of oxalate salts. Indeed, the interaction of matter with X-ray irradiation has been generally underestimated. Typically, X-ray induced damage has largely been considered as a poorly-understood nuisance. Only recently, investigations of electronic decay cascades that are triggered by the absorption of X-ray photons offered more insights into the mechanism of this process.[10-17] Essentially, the absorption of X-ray photons with the energies close to the K-shell energy excites core shell electrons to a bound state[11,14] or knocks them out from the host to the surrounding environment[10] and subsequently activates electronic relaxation processes. At the end of these electronic relaxation cascades, the molecular system becomes multiply ionized and contains many free electrons in its vicinity which leads to distortion and dissociation of molecular structure. If additional external factors are applied (i.e. high pressure, or temperature), the distorted system will undergo structural and chemical transformations with the formation of novel molecular systems.[18]

Our previous studies showed that under hard X-ray (≥ 7 keV) irradiation, strontium oxalate (SrC_2O_4) undergoes chemical transformations.[19] We proposed that the final product of decomposition reaction consists of strontium carbonate ($SrCO_3$) and CO-derived materials. It has been found that the decomposition reaction strongly depends on the X-ray energy and photon fluence, and by using the X-ray diffraction techniques as an experimental probe of decomposition, we established the appropriate experimental conditions for efficiently controlling this process.[20] We have observed a strong dependence/resonance of the decomposition reaction with the X-ray energy that appears to correlate with the K-edge of Sr^{2+} cations, suggesting that excitation of core electrons of cations leads to the destabilization of the neighbouring $C_2O_4^{2-}$ anions, and thereby to molecular dissociation, and further formation of novel product. Nevertheless, the detailed characterizations of

[a] *Department of Physics and Astronomy, University of Nevada Las Vegas (UNLV), Las Vegas, Nevada, 89154-4002, USA. *E-mail: evlyukhin_e.a@mail.ru*
[b] *Division of Geological and Planetary Sciences, California Institute of Technology, Pasadena, California 91125, U.S.A.*

†Electronic Supplementary Information (ESI) available: [details of any supplementary information available should be included here]. See DOI: 10.1039/x0xx00000x

composition and optical/electrical properties of the final products were still unclear.

Herein, the high pressure assisted X-ray induced decomposition of SrC_2O_4 is demonstrated and characterization of the final products by means of IR, XRD and UV-vis spectroscopy is discussed suggesting that the synthesized materials are novel amorphous Sr-based wide bandgap semiconductors. First, we studied the effect of high pressure (up to 10 GPa) on pure powders of SrC_2O_4 (Alfa Aesar, 95% purity) loaded in a diamond anvil cell (DAC) by means of XRD. Fig. 1a shows the in situ XRD patterns of SrC_2O_4 at selected pressure points (the full range of studied pressure is presented in Fig. S1 ESI†). The first XRD pattern obtained at ambient pressure matches the previously-reported monoclinic crystal structure of SrC_2O_4 with *C2/c* space group[21] (orange vertical bars in Fig. 1a).

Upon pressurization (up to 3 GPa), no changes in XRD patterns are observed indicating that SrC_2O_4 does not undergo any structural transformations. However, significant changes in the XRD pattern appear when sample is pressurized at 3.5 GPa. New peaks at 4.8 Å, 3.8 Å, and two peaks around 3.3 Å appear. Moreover, the peak at 3.06 Å from the original structure almost disappears and the peak at 2.8 Å splits into two. Nevertheless, as evident in Fig. 1a, most of the peaks from the original structure are still present in the XRD pattern at 3.5 GPa, suggesting that two different crystal structures coexist with each other at this pressure. Based on previously reported thermally induced phase transitions of barium oxalate,[22] we performed first-principles calculations to identify a new crystal structure of SrC_2O_4. The total energy calculations indicate a pressure induced monoclinic (*C2/c*) to triclinic (*P-1*) transition (see Fig. S4 ESI†). The calculated transition pressure from *C2/c* to *P-1* is predicted between 9-10 GPa. However, the energy difference between *C2/c* and *P-1* phases is less than 0.12 eV/f.u. or 0.02 eV/atom, implying the possible coexistence of both phases between 3-10 GPa as observed experimentally in XRD patterns. Fig. 1b displays the 3D structure of the theoretically-predicted triclinic crystal structure of SrC_2O_4 at pressure ≥ 3.5 GPa with space group *P-1* and lattice parameters a = 4.797 Å, b = 8.3763 Å, and c = 8.3899 Å (full assignment is presented in Fig. S3 ESI†). Both structures: original-monoclinic and new-triclinic coexist when SrC_2O_4 pressurized at 3.5 GPa as demonstrated in Fig. 1a (orange and purple vertical bars) and further pressurization (up to 10 GPa) does not significantly change the XRD patterns with the exception that the intensity of most peaks from the original structure decreases. Based on our results, the complete phase transformation of SrC_2O_4 is anticipated to appear above 10 GPa, however, the pressure study above this pressure point was not a scope of this work as all samples were synthesized in the 0–10 GPa pressure range, correspondingly.

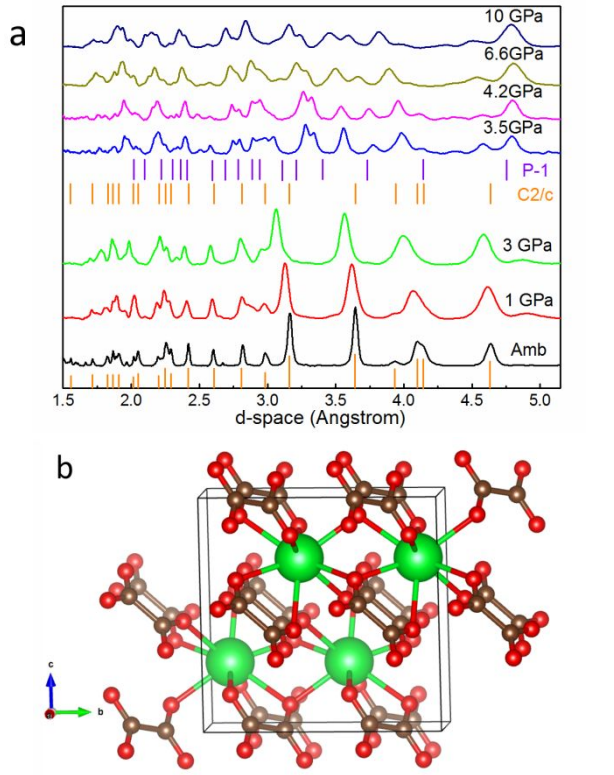

Fig. 1 (a) XRD patterns of SrC_2O_4 at selected pressure points up to 10 GPa. Orange vertical bars indicate peak positions of the monoclinic structure of strontium oxalate[21] and purple vertical bars correspond to the peak positions of the theoretically predicted triclinic crystal structure of SrC_2O_4 at pressures ≥ 3.5 GPa (the full XRD patterns assignment is presented in Fig. S2 and Fig. S3 ESI†). (b) Theoretically predicted triclinic crystal structure of SrC_2O_4 with *P-1* space group. Green, red and brown spheres represent Sr, O, and C atoms respectively.

X-ray induced synthesis of novel materials was performed at the High Pressure Collaborative Access Team's (HP-CAT's) 16 BM-B beamline at the Advanced Photon Source using "white" X-rays. For large volume samples (1×1 mm), starting materials were loaded into the high-pressure and temperature cell assembly which was then placed inside a large volume Paris-Edinburgh (PE) press equipped with tungsten carbide (WC) culets 3 mm in diameter for pressurization.[23,24] For small volume samples (40×100 µm), a symmetric-style DAC was used. All samples were synthesized at room temperature in the 0 to 10 GPa pressure range with 1 GPa steps via X-ray irradiation (90 min) using a beam ~1 mm in diameter. We note that X-ray induced decomposition depends on the sample thickness. Although, we observed that thin samples (~40 µm) at high pressure undergo chemical transformation even after 15 min of X-ray irradiation, larger volume samples require longer irradiation time. Thus, for consistency between different experiments, all samples were irradiated for 90 min at each pressure point. Fig. 2 displays several examples of the recovered products synthesized at different pressure points. Two samples synthesized at ambient pressure (Fig. 2a and d) are different from those obtained at high pressure (Fig. 2b, c, e, and f). Ambient-synthesized samples are yellow powders whereas high pressure fabricated products are glassy-type materials. All recovered samples are highly fluorescent using 514-532 nm laser irradiation and appear

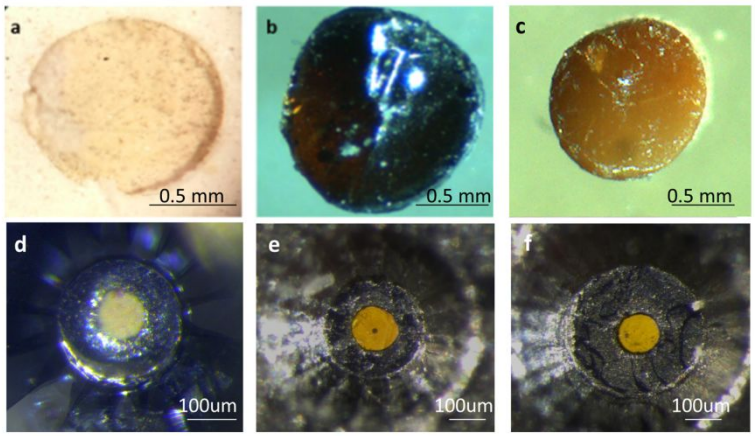

Fig. 2 Pictures of recovered products synthesized via X-ray irradiation at different pressure points in PE cells (top photos) and DAC (bottom photos). (a) PE sample at ambient pressure. (b) PE sample at 4 GPa. (c) PE sample at 10 GPa. (d) DAC sample at ambient. (e) DAC sample at 4 GPa. (f) DAC sample at 10 GPa.

different from their original pure SrC_2O_4 form which is a white powder.[19]

Moreover, XRD characterization of the final recovered products (obtained at high pressure) showed no evidence of material crystallinity suggesting that the obtained samples exhibit an amorphous nature. To support this idea, several recovered samples were heated for 24 hours at 300-400 °C which is below the decomposition temperature of SrC_2O_4 (420-590 °C)[25] but high above the glass transition temperature of Sr-based bulk metallic glasses.[26] No visible changes were observed and all of the heated samples were still highly fluorescent when using 514-532 nm laser irradiation, suggesting high chemical stability of the synthesized products.

To investigate the composition of the final products, Mid-IR spectroscopy was performed. Fig. 3a displays Mid-IR spectra of pure SrC_2O_4 and $SrCO_3$ at ambient pressure as well as spectra of recovered large volume samples synthesized at ambient pressure and at 1 GPa. The spectrum of the sample synthesized

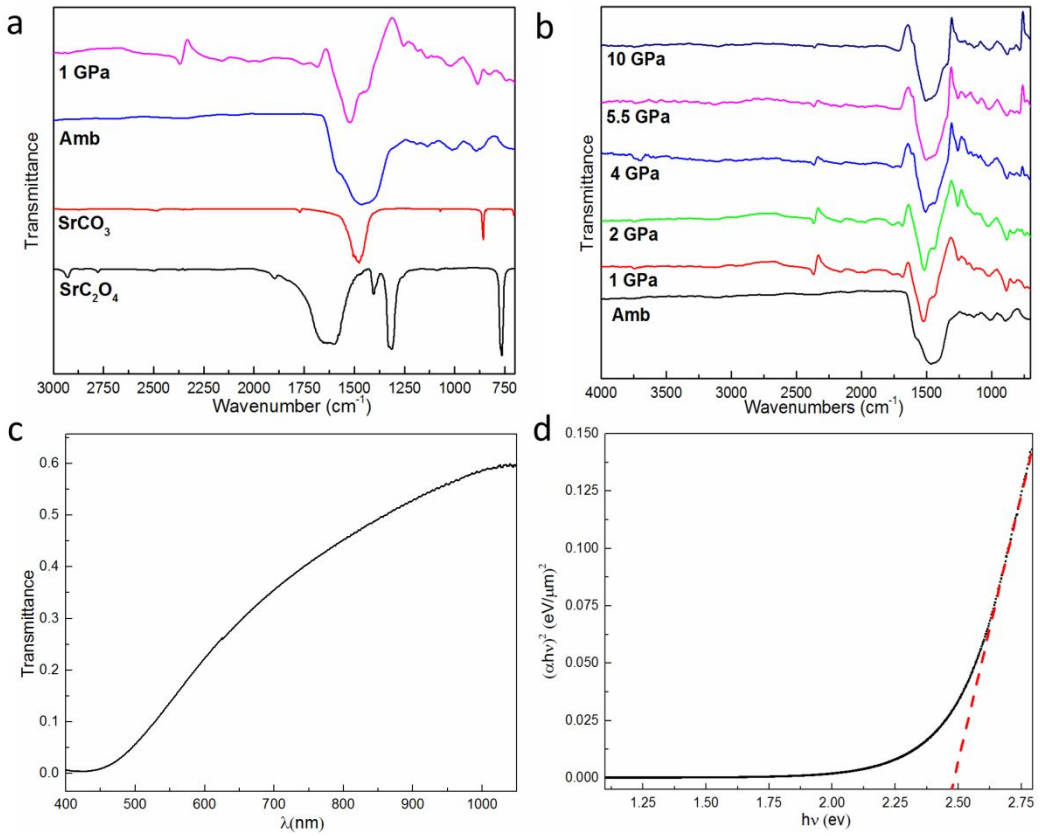

Fig. 3 (a) Mid-IR spectra of virgin samples of SrC_2O_4 and $SrCO_3$, and recovered synthesized products at ambient pressure and 1 GPa. (b) Mid-IR of recovered large volume (PE) samples synthesized at different pressures. (c) Transmission spectrum in the wavelength range from 400 to 1000 nm of the recovered small volume (DAC) sample synthesized at 1 GPa. (d) Variation of $(\alpha h\nu)^2$ vs photon energy $(h\nu)$ for the recovered small volume (DAC) sample synthesized at 1 GPa.

at ambient pressure possesses one strong peak at 1468 cm^{-1} which is also observed in the pure $SrCO_3$ spectrum and can be assigned to $\nu_d(CO)$[27] indicating that under X-ray irradiation at ambient pressure, SrC_2O_4 transforms to $SrCO_3$. The picture dramatically changes when the products are synthesized at high pressure. This can be observed in Fig. 3a where the spectrum of the sample synthesized at 1 GPa shows several characteristic bands at 885, 1255, 1435, 1524, 1677 and 2369 cm^{-1}. Bands at 885 and 1524 cm^{-1} can be assigned as $\pi(CO_3)$ and $\nu_d(CO)$ correspondingly[27] which are also observed in the pure $SrCO_3$ spectrum. The shoulder at 1435 cm^{-1} indicates a slight presence of undecomposed SrC_2O_4 and corresponds to the stretching modes of C-O and C-C groups[27]. The vibrational band at 2369 cm^{-1} corresponds to the CO_2 stretching mode[28,29] demonstrating that CO_2 is trapped inside the final product. It should be noted that Mid-IR spectroscopy was performed several months after the initial material synthesis and detection of CO_2 in the final products, suggesting that the obtained materials exhibit longterm CO_2-storage properties. The remaining vibrational bands at 1255 and 1677 cm^{-1} were previously observed in solid CO[28-30] and can be assigned as stretching motion of C-O-C or C-(C=O)-C and C=C groups, respectively, indicating the presence of CO-derived materials in our final product. Based on the obtained spectroscopic measurements, it is suspected that SrC_2O_4 subjected to high pressure and X-ray irradiation undergoes chemical transformations with the formation of $SrCO_3$ and CO-derived materials which could be potentially a new form of solid CO.

The next question we address in this work is the high pressure dependence of synthesized product's composition. Fig. 2b presents Mid-IR spectra of large volume samples obtained at different pressures. As is observed from the figure, increase of pressure reduces the intensity of some characteristic vibrational bands. The shoulder at 1435 cm^{-1}, which corresponds to vibrational bands of undecomposed SrC_2O_4, decreases with pressure increase suggesting that at higher pressure, the initial material mostly transforms to $SrCO_3$. This observation is supported by the intensity decrease of the CO_2 vibrational band at 2369 cm^{-1} and decrease of peaks at 1255 and 1677 cm^{-1} which potentially represent the presence of CO-derived materials in the final products. Therefore, we conclude that although high pressure is a necessary parameter for efficient synthesis of our novel materials, a pressure above 4 GPa (when virgin unirradiated SrC_2O_4 undergoes pressure-induced structural transformations) leads the X-ray induced decomposition reaction toward ambient decomposition when SrC_2O_4 transforms to $SrCO_3$. This apparent pressure dependence of decomposition may be explained by the coexistence of two crystal structures in the initial SrC_2O_4 powder pressurized ≥ 3.5 GPa (see Fig. 1a); therefore X-ray induced decomposition above 3.5 GPa likely proceeds differently from the decomposition reaction that occurs below this critical pressure.

The last question we address in this work pertains to the optical properties of synthesized products investigated by means of UV-vis spectroscopy. Indeed, the optical bandgap energy is a key parameter determining the material's range of most efficient operation in optical/electrical applications.[31,32] Polarized optical transmission spectra in the 350–1050 nm range were obtained for all recovered small volume samples synthesized in a DAC. Fig. 3c displays transmission spectra in the wavelength range from 400 to 1000 nm of the recovered sample obtained at 1 GPa. It can be seen from the figure that in the wavelength range above 1000 nm, the synthesized product exhibits high transmittance properties whereas in a lower wavelength range around 400 nm, it is almost opaque. The value of absorption coefficient *(α)* is calculated using the relation[31] $\alpha = \mu^{-1} \times ln(T^{-1})$, where μ is the sample thickness and T is the transmittance. The estimated value of α lies in between 0.14 - 0.001 μm^{-1}. The bandgap energy *(E_g)* has been calculated by using the Tauc relation[33,34] $(\alpha h\nu)^n = A(h\nu - E_g)$, where A is the edge parameter, h is the Plank's constant, $h\nu$ is the photon energy, α is the absorption coefficient and n is either 2 for direct band transitions or ½ for indirect band transitions.[35] The direct optical bandgap energy (see Fig. 3d) is estimated from a Tauc plot of $(\alpha h\nu)^2$ versus photon energy $h\nu$ according to Kubelka-Munk theory.[36] The value of photon energy extrapolated to $\alpha=0$ yields an absorption edge which corresponds to a bandgap energy, E_g. The obtained direct optical bandgap energy of the recovered samples lies between 2.45 and 2.53 eV (see Table S1 ESI†) which corresponds to 506 – 490 nm wavelength range respectively. Obtained bandgap values are smaller than bandgap energies of pure SrC_2O_4 (4.07 eV)[37] and $SrCO_3$ (3.17 eV)[38] suggesting that synthesized products are a novel type of Sr-based wide bandgap semiconductor. We suspect that the small difference (0.08 eV) of the bandgap values obtained for all recovered samples synthesised at various pressures is due to the similar behaviour of crystallinity loss occurred in all samples after X-ray irradiation even with the presence of the different amount of obtained components (different composition of the samples synthesized below and above 4 GPa) in the final products. Indeed, the strong reduction of the bandgap energy observed in the synthesized materials can be explained by a loss of crystallinity in the final products which leads to perturbation of the valence/conduction bands and new charge carrier transitions between electronic states become possible.[3] Additionally, the transmission/absorption properties demonstrated here of a new type of Sr-based wide bandgap semiconductor suggest that this novel material will find application in UV optoelectronic and photovoltaic devices.[39, 40]

In summary, a novel type of Sr-based wide bandgap semiconductor has been synthesized by means of X-ray irradiation with high-pressure assistance. The final product exhibits a relatively narrow bandgap (2.45-2.53 eV) and possesses high absorption properties in the UV range, suggesting high technological importance of this material in UV optoelectronic and photovoltaic applications. Additionally, the long term CO_2 storage properties of synthesized materials and their high stability make them potentially useful in gas-sequestration applications. Moreover, a novel method for the efficient synthesis of a low cost wide bandgap semiconductor in bulk has been proposed, which has a comparatively simpler synthetic approach to conventional fabrication methods.

Experimental methods.

We performed three irradiation experiments of strontium oxalate (SrC_2O_4) powder (Alfa Aesar, 95% purity). For investigation of the high-pressure-induced phase transition (up to 10 GPa) of pure SrC_2O_4, a symmetric-style diamond anvil cell (DAC) with 250 μm thick stainless-steel gaskets was employed to confine and pressurize samples. The diamonds utilized each had culets ~300 μm in diameter. All samples were loaded into gaskets with a ~140 μm diameter hole that was drilled via electric discharge machining in the gasket center that was preindented to ~40 μm thickness. A methanol–ethanol (4:1) mixture was used as a pressure-transmitting medium.[41] A ruby sphere was loaded with the sample for pressure measurement purposes. X-ray induced synthesis of novel materials was performed at the High Pressure Collaborative Access Team's (HP-CAT's) 16 BM-B beamline at the Advanced Photon Source using "white" X-rays. For large volume samples (1×1 mm), starting materials were loaded into the high-pressure and temperature cell assembly which was then placed inside a large volume Paris-Edinburgh (PE) press equipped with tungsten carbide (WC) culets 3 mm in diameter for pressurization. For small volume samples (40×100 μm), a symmetric-style DAC was used. All samples were synthesized at room temperature in the 0 to 10 GPa pressure range with 1 GPa steps via X-ray irradiation (90 min) using a beam ~1 mm in diameter.

X-ray diffraction measurements were performed at the 16 BM-D beamline of the High Pressure Collaborative Access Team's (HP-CAT's) at the Advanced Photon Source. A tunable Si (111) double crystal in pseudo-channel-cut mode was used as a monochromator to filter "white" X-ray radiation and deliver X-rays of fixed but settable energies. Angular-dispersive X-ray diffraction patterns were collected using Mar345®image plate detector. Each diffraction pattern was collected for 1 minute at 25-32 keV X-ray energies. The horizontal and vertical full width half-maximum (FWHM) of the X-ray beam was 3.3 μm. The diffraction patterns were integrated in d-space using the Dioptas®program.[42]

Infrared spectroscopy analysis

The recovered large volume samples synthesized using PE press were individually interrogated via infrared spectroscopy. IR spectra were recorded at the Canadian Light Source (CLS). All spectral determinations were performed at room temperature and ambient pressure. At the CLS, mid-IR spectra were acquired at the 01B1-1 beamline using a Bruker Vertex 77 v/S, Hyperion 3000®IR microscope. A liquid Nitrogen-cooled MCT detector was used. The mid-IR microscope system typically focuses the IR beam which is then spatially filtered using 100 μm diameter circular aperture. The investigated spectral range was from 700 to 4000 wavenumbers with a resolution of 1 cm^{-1}. An improvised jacket that surrounded the sample and fit snugly between the objective and sample stage of microscope with constantly flowing argon gas was used to reduce water vapor contamination.

For comparison purposes the IR spectra of virgin SrC_2O_4 and $SrCO_3$ (Sigma Aldrich, 99.9% purity) were interrogated using a Shimadzu IRAffinity-1® spectrometer.

Polarized optical transmission spectra in the 350–1050 nm range were obtained at about 1 nm resolution with a home-built microspectrometer system consisting of a 1024 element Si- and a 256 element InGaAs diode-array detector coupled to a grating spectrometer system attached via fiber optics to a highly modified NicPlan infrared microscope containing a calcite polarizer.[43]

Computational methods.

First-principles total energy calculations were performed using spin-polarized density functional theory (DFT), as implemented in the Vienna ab initio simulation package (VASP).[44] The exchange-correlation energy was calculated using the generalized gradient approximation (GGA), with the parametrization of Perdew, Burke, and Ernzerhof (PBE).[45,46] The interaction between valence electrons and ionic cores was described by the projector augmented wave (PAW) method.[47] The Kohn-Sham (KS) equation was solved using the blocked Davidson[48] iterative matrix diagonalization scheme followed by the residual vector minimization method. The plane-wave cutoff energy for the electronic wavefunctions was set to a value of 500 eV, ensuring the total energy of the system to converge within 1 meV/atom. Electronic relaxation was performed with the conjugate gradient method accelerated using the Methfessel-Paxton Fermi-level smearing[49] with a Gaussian width of 0.1 eV. Ionic relaxation was carried out using the quasi-Newton method and the Hellmann-Feynman forces acting on atoms were calculated with a convergence tolerance set to 0.01 eV/Å. A periodic unit cell approach was used in the calculations. Structural relaxation was performed without symmetry constraints. The Brillouin zone was sampled using the Monkhorst-Pack k-point scheme[50] with 5×5×5 k-point meshes in all the calculations.

Conflicts of interest

There are no conflicts to declare.

Acknowledgements

We gratefully acknowledge support from the Department of Energy National Nuclear Security Administration (DOE-NNSA) under Award Number DE-NA0002912. We also acknowledge support from the DOE Cooperative Agreement No. DE-FC08-01NV14049 with the University of Nevada, Las Vegas. Portions of this work were performed at HPCAT (Sector 16), Advanced Photon Source (APS), Argonne National Laboratory. HPCAT operation is supported by DOE-NNSA under Award No. DE-NA0001974, with partial instrumentation funding by NSF. The Advanced Photon Source is a U.S. Department of Energy (DOE) Office of Science User Facility operated for the DOE Office of Science by Argonne National Laboratory under Contract No. DE-AC02-06CH11357. A portion of the research described in this paper was performed at the Mid-IR beamline of the Canadian Light Source, which is supported by the Natural Sciences and Engineering Research Council of Canada, the National Research Council Canada, the Canadian Institutes of Health Research, the

Province of Saskatchewan, Western Economic Diversification Canada, and the University of Saskatchewan

References

1 K. Morigaki and C. Ogihara, in *Springer Handbook of Electronic and Photonic Materials*, ed. S. Kasap and P. Capper, Springer International Publishing, New York, 2, 2017, 25, 565-580.
2 N. F. Mott, *Conduction in non-crystalline materials*, Oxford Science Publication, Oxford, 1987.
3 A. Walsh, J. L. F. Da Silva and S.-H. Wei, *Chem. Mater.*, 2009, **21**, 5119.
4 C. Feldman, and K. Moorjani, *APL Tech. Dig.,* 1968, **7**, 2.
5 D. Adler, H. K. Henisch and S. N. Mott, *Rev. Mod. Phys.,* 1978, **50**, 209.
6 H. Fritzsche and S. R. Ovshinsky, *J. Non-Cryst. Solids*, 1970, **2**, 393.
7 H. Hosono, N. Kikuchi, N. Ueda and H. Kawazoe, *J. Non-Cryst. Solids*, 1996, **198-200**, 165.
8 U. Noriyuki, K. Hiroshi, M. Yusuke, T. Tetsuya and K. Toshihiko, *Appl. Phys. Express*, 2008, **1**, 121502.
9 B. Abeles and T. Tiedje, *Phys. Rev. Lett.*, 1983, **51**, 2003.
10 V. Stumpf, K. Gokhberg and L. S. Cederbaum, *Nat. Chem.*, 2016, **8**, 237.
11 F. Trinter, M. S. Schöffler, H. K. Kim, F. P. Sturm, K. Cole, N. Neumann, A. Vredenborg, J. Williams, I. Bocharova, R. Guillemin, M. Simon, A. Belkacem, A. L. Landers, T. Weber, H. Schmidt-Böcking, R. Dörner and T. Jahnke, Nature, 2013, **505**, 664.
12 S. Thürmer, M. Ončák, N. Ottosson, R. Seidel, U. Hergenhahn, S. E. Bradforth, P. Slavíček and B. Winter, *Nat. Chem.,* 2013, **5**, 590.
13 L. S. Cederbaum, J. Zobeley and F. Tarantelli, *Phys. Rev. Lett.*, 1997, **79**, 4778.
14 K. Gokhberg, P. Kolorenč, A. I. Kuleff and L. S. Cederbaum, Nature, 2013, **505**, 661.
15 T. Jahnke, *J. Phys. B: At. Mol. Opt. Phys.,* 2015, **48**, 082001.
16 T. Jahnke, H. Sann, T. Havermeier, K. Kreidi, C. Stuck, M. Meckel, M. Schöffler, N. Neumann, R. Wallauer, S. Voss, A. Czasch, O. Jagutzki, A. Malakzadeh, F. Afaneh, T. Weber, H. Schmidt-Böcking and R. Dörner, *Nat. Phys.*, 2010, **6**, 139.
17 J. Zobeley, R. Santra and L. S. Cederbaum, *J. Chem. Phys.*, 2001, **115**, 5076.
18 E. Evlyukhin, E. Kim, D. Goldberger, P. Cifligu, S. Schyck, P. F. Weck and M. Pravica, *Phys. Chem. Chem. Phys.,* 2018**, 20,** 18949.
19 M. Pravica, E. Evlyukhin, P. Cifligu, B. Harris, J. Jae Koh, N. Chen and Y. Wang, *Chem. Phys. Lett.*, 2017, **686**, 183.
20 D. Goldberger, E. Evlyukhin, P. Cifligu, Y. Wang and M. Pravica, *J. Phys. Chem. A*, 2017, **121**, 7108.
21 D. J. Price, A. K. Powell and P. T. Wood, *Polyhedron*, 1999, **18**, 2499.
22 A. N. Christensen, L. M. Arnbjerg, E. DiMasi, Y. Cerenius, B. C. Hauback and T. R. Jensen, *Solid State Sci.*, 2011, **13**, 1407.
23 Y. Kono, C. Park, T. Sakamaki, C. Kenny-Benson, G. Shen and Y. Wang, *Rev. Sci. Instrum.*, 2012, **83**, 033905.
24 A. Yamada, Y. Wang, T. Inoue, W. Yang, C. Park, T. Yu and G. Shen, *Rev. Sci. Instrum.*, 2011, **82**, 015103.
25 E. Knaepen, J. Mullens, J. Yperman and L. C. Van Poucke, *Thermochim. Acta*, 1996, **284**, 213.
26 K. Zhao, W. Jiao, J. Ma, X. Q. Gao and W. H. Wang, *J. Mater. Res.,* 2012, **27**, 2593.
27 E. D. Bacce, A. M. Pires, M. R. Davalos and M. Jafelicci Jr, *Int. J. Inorg. Mater.*, 2001, **3**, 443.
28 W. J. Evans, M. J. Lipp, C. S. Yoo, H. Cynn, J. L. Herberg, R. S. Maxwell and M. F. Nicol, *Chem. Mater.*, 2006, **18**, 2520.
29 M. Ceppatelli, A. Serdyukov, R. Bini and H. J. Jodl, *J. Phys. Chem. B*, 2009, **113**, 6652.
30 M. J. Lipp, W. J. Evans, B. J. Baer and C.-S. Yoo, *Nat. Mater.,* 2005, **4**, 211.
31 Triloki, R. Rai and B. K. Singh, *Nucl. Instrum. Methods Phys. Res. A*, 2015, **785**, 70.
32 R. Köferstein, L. Jäger and S. G. Ebbinghaus, *Solid State Ion.,* 2013, **249-250**, 1.
33 J. Tauc, *Mater. Res. Bull.,* 1968, **3**, 37.
34 J. Tauc, R. Grigorovici and A. Vancu, *Phys. Status Solidi B*, 1966, **15**, 627.
35 S. Tsunekawa, T. Fukuda and A. Kasuya, *J. Appl. Phys.,* 2000, **87**, 1318.
36 A. K. Alexander, *J. Phys. D: Appl. Phys.*, 2007, **40**, 2210.
37 P. Dalal, V., Deshpande, M., P., *Int. J. Phys. and Astron.,* 2014, **2**, 129.
38 S. Ni, X. Yang and T. Li, *Mater. Lett.*, 2011, **65**, 766.
39 E. Fortunato, D. Ginley, H. Hosono and D. C. Paine, *MRS Bull.*, 2011, **32**, 242.
40 E. Monroy, F. Omnès and F. Calle, *Semicond. Sci. Technol.,* 2003, **18**, 33.
41 S. Klotz, J. C. Chervin, P. Munsch, and G. L. Marchand, *J. Phys. D: Appl. Phys.*, 2009, **42**, 075413.
42 C. Prescher and V. B. Prakapenka, *High Press. Res.*, 2015, **35**, 223.
43 G. R. Rossman and M. N. Taran, *Am. Mineral.,* 2001, **86**, 896.
44 G. Kresse and J. Furthmüller, *Phys. Rev. B,* 1996, **54**, 11169.
45 J. P. Perdew, J. A. Chevary, S. H. Vosko, K. A. Jackson, M. R. Pederson, D. J. Singh, and C. Fiolhais, *Phys. Rev. B,* 1992, **46**, 6671.
46 J. P. Perdew, K. Burke, and M. Ernzerhof, *Phys. Rev. Lett.,* 1996, **77**, 3865.
47 P. E. Blöchl, *Phys. Rev. B,* 1994, **50**, 17953.
48 E. R. Davidson, *Methods in Computational Molecular Physics,* Plenum, New York,1983.
49 M. Methfessel and A. T. Paxton, *Phys. Rev. B,* 1989, **40**, 3616.
50 H. J. Monkhorst and J. D. Pack, *Phys. Rev. B,* 1976, **13**, 5188.

Graphical abstract

Synthesis of a novel strontium-based wide-bandgap semiconductor via X-ray photochemistry at extreme conditions.

Egor Evylukhin[1]*, Eunja Kim[1], Petrika Cifligu[1], David Goldberger[1], Sarah Schyck[1], Blake Harris[1], Sindi Torres[1], George R. Rossman[2], Michael Pravica[1]

[1]Department of Physics and Astronomy, University of Nevada Las Vegas (UNLV), Las Vegas, Nevada, 89154-4002, USA
[2]Division of Geological and Planetary Sciences, California Institute of Technology, Pasadena, California 91125, USA

Synthesis of Sr-based wide bandgap semiconductor has been demonstrated via X-ray irradiation of strontium oxalate at high pressure.